Robust Incremental State Estimation through Covariance Adaptation

Ryan M. Watson[1], Jason N. Gross[1], Clark N. Taylor[2], and Robert C. Leishman[2]

***Abstract*—Recent advances in the fields of robotics and automation have spurred significant interest in robust state estimation. To enable robust state estimation, several methodologies have been proposed. One such technique, which has shown promising performance, is the concept of iteratively estimating a Gaussian Mixture Model (GMM), based upon the state estimation residuals, to characterize the measurement uncertainty model. Through this iterative process, the measurement uncertainty model is more accurately characterized, which enables robust state estimation through the appropriate de-weighting of erroneous observations. This approach, however, has traditionally required a batch estimation framework to enable the estimation of the measurement uncertainty model, which is not advantageous to robotic applications. In this paper, we propose an efficient, incremental extension to the measurement uncertainty model estimation paradigm. The incremental covariance estimation (ICE) approach, as detailed within this paper, is evaluated on several collected data sets, where it is shown to provide a significant increase in localization accuracy when compared to other state-of-the-art robust, incremental estimation algorithms.**

I. Introduction

The ability to infer information about the system and the operating environment is one of the key components enabling many robotic applications. To equip robotic platforms with this capability, several state estimation frameworks [1] have been developed (e.g., the Kalman filter [2], or the particle filter [3]).

The traditional state estimation methodologies perform adequately when the collected observations adhere to the *a priori* models. However, in many robotic applications of interest, the observations can be degraded (e.g., global navigation satellite system (GNSS) observations in an urban environment, or RGB observations in a low-light setting), which cause a deviation between the collected observations and the assumed models. When this deviation is present, the traditional state estimation schemes (i.e., estimators that utilize the l^2-norm exclusively to construct the cost-function) can breakdown [4].

To overcome the breakdown of traditional state estimators in data degraded scenarios, several robust estimation schemes have been developed. These robust estimation schemes compensate for erroneous observations by either adapting the measurement function [5], [6] or by adapting the measurement uncertainty model [7]. As discussed within [8], there is an equivalence between these two compensation schemes. Thus, within this work, the focus will be on erroneous observation compensation though measurement uncertainty model adaptation.

To enable this measurement uncertainty model adaptation in practice, several implementations have been developed. Specifically, these implementations fall into one of two paradigms. The methods that fall into the first framework are the group of consensus seeking (i.e., the approaches that conduct optimization with a trusted subset of the original observations) approaches (e.g., realizing, reversing, recovering (RRR) [9], single-cluster spectral graph partitioning (SCGP) [10], and l^1 relaxation [11]). The methods that fall into the second framework are the group of de-weighting (i.e., the approaches that conduct optimization with all the observations; however, they remain robust by reducing the contribution of observations based upon their deviation from the assumed model) approaches (e.g., maximum likelihood type estimators (m-estimators) [7], switchable constraints [12], and dynamic covariance scaling (DCS) [13]).

To extend the robust state estimation through covariance adaptation approach from the traditional uni-modal uncertainty model paradigm to a multi-modal implementation, the max-mixtures (MM) [14] approach was developed. The MM approach mitigates the increased computation complexity generally assumed to accompany the incorporation of multi-modal uncertainty models by first assuming that the uncertainty model can be represented by a Gaussian mixture model (GMM), then selecting the single Gaussian component from the GMM that maximizes the likelihood of the individual observation given the current state estimate.

When initially proposed, the MM approach utilized a static measurement uncertainty model (i.e., the multi-modal measurement uncertainty model is assumed known *a priori*). To extend the MM approach to scenarios where the measurement uncertainty model is not accurately characterized *a priori*, several works [15]–[17] have investigated the concept of adapting the measurement uncertainty model based upon the state estimation residuals [18].

Through this adaptive process, the measurement uncertainty model is more accurately characterized, which enables robust state estimation through the appropriate de-weighting of erroneous observations. This approach, however, has traditionally required a batch [19], or fixed-lag [20] estimation framework to enable the estimation of the measurement uncertainty model, which is not advantageous to most robotic applications, as incremental updates are usually required. Additionally, as we'll discuss in this paper, theses approaches are inefficient – both respect to memory and computation – in the estimation of the measurement uncertainty model.

[1]Department of Mechanical and Aerospace Engineering, West Virginia University, Morgantown, WV
[2]Autonomy and Navigation Technology Center, Air Force Institute of Technology

Within this paper, we propose a novel extension to the measurement uncertainty model estimation paradigm. Specifically, we propose an efficient, incremental extension of the methodology. The efficiency of the approach is granted by incrementally adapting the uncertainty model with only a small subset of informative state estimation residuals (i.e., the state estimation residuals which do not adhere to the *a priori* model), which is a key differentiating factor between the proposed approach and those previously developed [15], [20]. The incremental nature of the approach is granted through recent advances within the probabilistics graphical model community (i.e., through the utilization of the incremental smoothing and mapping (iSAM2) [21] algorithm), in conjunction with the ability to merge GMM's [22].

To provide a discussion of the proposed incremental covariance estimation (ICE) approach, the remainder of the paper is accordingly organized. First, a brief introduction to state estimation is provided in Section II, with a specific emphasis being placed on the current limitations of robust state estimation. Based upon the discussion provided in Section II, the discussion turns to the proposed ICE robust framework in Section III. In Section IV, the proposed ICE approach is validated on several collected GNSS data sets, where improved estimation accuracy is observed, when compared to other state-of-the-art robust state estimators. Finally, the paper terminates in Section V with a brief conclusion and discussion of future research.

II. State Estimation

A. Batch Estimation

For the sake of completeness, a succinct review of state estimation and its robust variants is detailed in this section. For a more thorough examination of the topic, the reader is referred to Section II of [19].

To begin, the general state estimation problem can be formulated as the process of inferring a set of states X that – in some sense – are in best agreement with the provided information Y. The metric utilized to quantify agreement, in this work, is the maximization of the *posterior* distribution (i.e., the maximum a posteriori (MAP) state estimate $\hat{X}$), as presented in Eq. 1.

$$\hat{X} = \underset{X}{\operatorname{argmax}} \ \ \mathrm{p}(X \mid Y) \tag{1}$$

To enable the implementation of the MAP estimation problem, the factor graph [23] formulation can be utilized. The factor graph is a probabilistic graphical model framework which enables the factorization of the *posterior* distribution into a product of functions that operate on a reduced domain, as shown in Eq. 2

$$\mathrm{p}(X \mid Y) \propto \prod_{n=1}^{N} \psi_n(A_n, B_n), \tag{2}$$

where, $\psi_n(A_n, B_n)$ is an application specific domain reduced function (i.e., a factor in the factor graph model), which operates on $A_n \subseteq \{X_1, X_2 \ldots, X_n\}$, and $B_n \subseteq \{Y_1, Y_2 \ldots Y_m\}$.

When utilizing the factor graph formulation, as a means to enable a computationally efficient implementation, it is commonly assumed that each factor within the factorization adheres to a Gaussian noise model. With this assumption in place, the estimation problem presented in Eq. 1 is reduced to finding the set of states which minimizes the squared sum of weighted residuals [24], as presented in Eq. 3

$$\hat{X} = \underset{X}{\operatorname{argmin}} \sum_{n=1}^{N} || \ r_n(X) \ ||_{\Lambda_n} \quad \text{s.t.} \quad r_n(X) \triangleq y_n - h_n(X), \tag{3}$$

where $r_n(X)$ is an observation residual, h_n is a function that maps the state estimate to the observation domain, Λ_n is the utilized covariance (i.e., residual weighting) matrix, and $|| * ||$ is defined as the l^2-norm.

B. Incremental Estimation

For many applications, the information is provided incrementally. When this is the case, the estimation framework discussed previously is inefficient due to the need to refactor the entire measurement Jacobian matrix every time a new information is provided.

To overcome this computation limitation, the concept of incrementally updating the matrix factorization (e.g., QR-decomposition) was studied within [25]. Within [25], they enabled the incremental updating of the matrix factorization by first augmenting the previous factorization, then, restoring the upper triangular form of the factorization through the utilization of Givens rotations[1].

The approach proposed within [25] does have one key limitation, which is the requirement to conduct periodic batch re-computation of the QR-decomposition for the entire measurement Jacobian matrix to enable variable re-ordering. This batch re-computation is utilized to maintain the sparsity of the upper-triangular system. To mitigate this batch re-computation the Bayes tree [27] was introduced. This directed graphical model directly represents the square root information matrix and can be easily computed from the associated factor graph in a two-step process, as detailed in [21]. Due to the structure of the Bayes tree graphical model, this methodology removes the requirement to re-factor the entire system when new information is added. Instead, only the affected section of the Bayes tree is re-factored, as detailed within [21]. This approach to state estimation is titled iSAM2, and is the approach utilized within this study.

C. Robust Estimation

Utilizing the iSAM2 approach provides an efficient estimation framework when the provided information adheres to the *a priori* models. However, when the provided information does not adhere to the *a priori* models, the estimator can breakdown

All software developed to enable the evaluation presented in this study is publicly available at **https://github.com/wvu-navLab/ICE**.

[1]See section 5.1.8 of [26] for a thorough review of Givens rotations with applications to least squares (LS).

[4]. This property is not exclusive to the iSAM2 framework, instead, it is a fundamental property of any estimation framework that exclusively utilizes the l^2-norm to construct its cost function.

To overcome this limitation, several robust estimation frameworks have been proposed (e.g., m-estimators [7], switchable constraints [12], and MM [14]). Linking all of these estimation frameworks is the concept of enabling robust estimation through appropriately weighting (i.e., scaling the assumed covariance model) the contribution of each information source based upon the level of adherence between the information and the *a priori* model. To implement this concept, the iteratively re-weighted least squares (IRLS) formation [28], as provided in Eq. 4, can be utilized, where the weighting function $w(*)$ is dependent upon the utilized robust estimation framework (e.g., DCS [13]).

$$\hat{X} = \underset{X}{\operatorname{argmin}} \sum_{n=1}^{N} w_n(e_n)\ e_n \quad \text{s.t.} \quad e_n \triangleq \|r_n(X)\|_{\Lambda_n} \tag{4}$$

To extend robust state estimation from the traditional uni-modal uncertainty model paradigm to a multi-modal implementation, the MM [14] approach was developed. The MM approach mitigates increased computation complexity generally assumed to accompany the incorporation of multi-modal uncertainty models by first assuming that the uncertainty model can be represented by a GMM, then selecting the single Gaussian component from the GMM that maximizes the likelihood of the individual observation given the current state estimate.

The MM approach was extended within the batch covariance estimation (BCE) framework [15], [19] to enable the estimation of the multi-modal covariance models during optimization. The BCE approach enables the estimation of the multi-modal covariance model through the utilization of variational inference (VI) [29] on the current set of state estimation residuals. The BCE approach provided promising results with the primary limitation being the batch estimation nature of the framework. To overcome this computational limitation, an extension to the BCE approach, as described within section III, which enables efficient incremental updating while maintaining the robust characteristics, is proposed within this paper.

III. Proposed Approach

To facilitate a discussion of the proposed ICE framework the assumed data model is first explained. Then, a method for incremental measurement uncertainty model adaptation is presented. Finally, pull the previously mentioned topics together, the discussion concludes with an overview of the proposed ICE framework.

A. Data Model

As calculated by the estimator, a set of state estimation residuals $\mathbf{R} = \{r_1, r_2, \ldots, r_N \mid r_n \triangleq y_n - h_n(X)\}$ is provided. The set of state estimation residuals can be characterized by a GMM, which, for this work, will act as the measurement uncertainty model, GMM_g. As proposed within [14], with the intent to minimize the computation complexity of the optimization problem, the GMM can be reduced to selecting the most likely component from the mixture model to approximately characterize each observation, as depicted in Eq. 5 where μ_m is the components mean and Λ_m is the components covariance.

$$r_n \sim \max_m w_m \mathcal{N}(r_n \mid \theta_m) \quad \text{s.t.} \quad \theta_m \triangleq \{\mu_m, \Lambda_m\} \tag{5}$$

For this work, it is additionally assumed that the set of residuals, $\mathbf{R}$, can be partitioned into two distinct groups. The first group is the set of all residuals which sufficiently adhere to the *a priori* covariance model (i.e., do not deviate sufficiently from the most likely component within GMM_g), which will be indicated by the set $\mathbf{R_I}$. While, the second group is the set residuals which do not sufficiently adhere to the *a priori* covariance model, which will be indicated by the set $\mathbf{R_O}$.

To quantify the level of adherence to the *a priori* uncertainty model, the $\mathrm{z\text{-}test}$, as provided in Eq. 6, is employed. Within Eq. 6 μ, and σ are the mean and standard deviation of the most likely component from GMM_g for the state estimation residual r_n. Utilizing the $\mathrm{z\text{-}test}$ as a metric to quantify the level of agreement between the set of state estimation residual and the *a priori* uncertainty model, we can more concretely define the two groupings as, $\mathbf{R_I} = \{r \mid r \in \mathbf{R},\ Z(r, \phi) < T_r\}$[2] and $\mathbf{R_O} = \{r \mid r \in \mathbf{R},\ r \notin \mathbf{R_I}\}$.

$$Z(r_n, \phi) = \frac{r_n - \mu}{\sigma} \quad \text{s.t.} \quad \phi \triangleq \{\mu, \sigma\} \tag{6}$$

B. Uncertainty Model Adaptation

By definition, the set $\mathbf{R_O}$ is not accurately characterized by GMM_g thus, it is desired to adapt the uncertainty model to more accurately represent the new observations. To enable the adaptation of the uncertainty model, a two step procedure is utilized. This procedure starts by estimating a new GMM, which will be indicated by GMM_n, based solely on the set $\mathbf{R_O}$. Then, GMM_n is merged into the prior model (i.e., GMM_g) to provide a more accurate characterization the measurement uncertainty model. This procedure is elaborated upon in Section III-B1 and Section III-B2, respectively.

1) Variational Clustering: To estimate GMM_n, the set of model parameters which maximizes the $\mathrm{log\ marginal\ likelihood}$, as depicted in Eq. 7, must be calculated. In Eq. 7, $\boldsymbol{\theta}$ is the set of mean vectors and covariance matrices which define the new GMM, and $\mathbf{Z}$ is an assignment variable (i.e., the variable $\mathbf{Z}$ assigns each $r \in \mathbf{R_O}$ to a specific component within the model).

$$\log \mathrm{p}(\mathbf{R_O}) = \log \int \mathrm{p}(\mathbf{R_O}, \boldsymbol{\theta}, \mathbf{Z}) d\mathbf{Z} d\boldsymbol{\theta} \tag{7}$$

In general, the integral presented in Eq. 7 is computational intractable [30]. Thus, a method of approximate integration

[2] T_r is a user defined parameter that encodes the acceptable amount an observation can deviation from the *a priori* model in terms of multiples of the standard deviation. For the evaluation presented, the 3-σ heuristic (i.e.,$T_r = 3.0$) was utilized to encode the acceptable amount of deviation.

must be implemented. For this work, the VI[3] [30], [31] approach is utilized primarily due this class of algorithms run-time performance when compared to sampling based approaches (i.e., Monte Carlo methods [32]).

To enable a VI based approximation, several parameters must be defined *a priori* (e.g., the prior distribution over the model parameters $\boldsymbol{\theta}$). The specific instantiation of VI utilized in the ICE algorithm is adopted from the previously proposed BCE approach. Thus, we have omitted a detailed discussion of the utilized inference approach within this article, as a discussion of the utilized VI approach is already detailed in Section III.A of [19].

2) Efficient GMM Merging: To enable the second step of the measurement uncertainty model adaptation (i.e., the merging of GMM_n into the prior model GMM_g), an implementation of the algorithm presented in [22] is utilized. To provide a description of the approach, let's evaluate the equivalence between $g_n \triangleq \{w_n, \mu_n, \Lambda_n\} \in \text{GMM}_n$ (e.g., the first component in GMM_n) and $g_g \triangleq \{w_g, \mu_g, \Lambda_g\} \in \text{GMM}_g$ (e.g., the first component in GMM_g).

To test the equivalence, we will first extract the set of observations $\mathbf{R}_{\mathbf{O},\mathbf{g_n}} \subseteq \mathbf{R_O}$ that correspond to set of state estimation residuals that are characterized by component g_n. Utilizing $\mathbf{R}_{\mathbf{O},\mathbf{g_n}}$, it is desired to check if the set of state estimation residuals has an equivalent covariance to the hypothesis covariance model (i.e., we want to see if $\Lambda_n = \Lambda_g$, where $\Lambda_n = \text{cov}(\mathbf{R}_{\mathbf{O},\mathbf{g_n}})$ and Λ_g is the hypothesis covariance from g_g).

To determine if our two GMM components have an equivalent covariance model, we must first transform the set of observations $\mathbf{R}_{\mathbf{O},\mathbf{g_n}}$ with Cholesky decomposition of our hypothesis covariance[4]. This transformation provides us with a new data set, defined as $\mathbf{Y} = \{y = L^{-1}r \mid r \in \mathbf{R}_{\mathbf{O},\mathbf{g_n}},\ \Lambda_g = LL^T\}$.

Utilizing the transformed set of state estimation residuals $\mathbf{Y}$, the W-statistic [33] can be constructed, as provided in Eq. 8, to test the equivalence of covariance matrices. Within Eq. 8, $\Lambda_y = \text{cov}(\mathbf{Y})$, m is the cardinality of the set $\mathbf{Y}$ (i.e., $m = |\mathbf{Y}|$), and d is the dimension the state estimation residuals (i.e, $y_m \in \mathbb{R}^d$).

$$W = \frac{1}{d}Tr\big((\Lambda_y - I)^2\big) - \frac{d}{m}\big(\frac{1}{d}Tr(\Lambda_y)\big)^2 + \frac{d}{m} \tag{8}$$

The W-statistic is known to have an asymptotic χ^2 distribution with degrees of freedom $d(d+1)/2$, as depicted in Eq. 9. Thus, a Chi-square test with a user defined critical value is utilized to test the equivalence of covariance matrices.

$$\frac{mWd}{2} \sim \chi^2_{d(d+1)/2} \tag{9}$$

To test the equivalence of mean vectors, the T-statistic [34], as provided in Eq. 10, is utilized. Within Eq. 10, μ_n is the mean of the component of GMM_n, and μ_g is the mean vector of the component of GMM_g. The T-statistic is utilized to test the equivalence of mean vectors because it is known to have an asymptotic F distribution, as depicted in Eq. 11. Thus, an F-test with user defined critical value is utilized to test the equivalence of mean vectors.

$$T^2 = m\left\|\mu_n - \mu_g\right\|_{\Lambda_y} \tag{10}$$

$$\frac{m-d}{d(m-1)}T^2 \sim F_{d,m-d} \tag{11}$$

If both the mean and covariance of two components are found to be equivalent, then the new component g_n is merged with the prior component g_g to adapt the measurement uncertainty model GMM_g. To adapt the measurement uncertainty model, the mean, covariance and weighting can be updated, as presented in Eqs. 12, 13, and 14, respectively. Within Eqs. 12, 13, and 14, N is the total number of points which are characterized by GMM_g, M is the total number of points which are characterized by GMM_n, and m is the number of points which are characterized by component g_n.

$$\mu = \frac{Nw_g\mu_g + m\mu_n}{Nw_g + m} \tag{12}$$

$$\Lambda = \frac{Nw_g\Lambda_g + m\Lambda_n}{Nw_g + m} + \frac{Nw_g\mu_g\mu_g^T + m\mu_n\mu_n^T}{Nw_g + m} - \mu\mu^T \tag{13}$$

$$w = \frac{Nw_g + m}{N + M} \tag{14}$$

If the new component g_n does not match a component within GMM_g, then the mean and covariance of g_n is added to GMM_g. When the new component is added to GMM_g the weighting vector is updating, as presented in Eq. 15, where N, M, and m are as defined above. When the new component is added, the weighting for all of the remaining components in GMM_g are updated according to Eq. 16.

$$w = \frac{m}{N + M} \tag{15}$$

$$w = \frac{Nw_g}{N + M} \tag{16}$$

Through the utilization of the mixture model merging approach developed within [22], and outlined in this section, the measurement uncertainty model can be adapted online. This adaptation is conducted without the need for storing all previous state estimation residuals (i.e, only the most recent residuals $\mathbf{R_O}$ which do not adhere to the *a priori* model are required), which dramatically reduces the computational and memory cost of the proposed approach.

C. Algorithm Overview

With the discussion provided in the previous sections, the conversation can now turn to an overview of the proposed robust estimation framework. To facilitate a discussion, a graphical overview of the ICE framework is depicted in Fig. 1.

From Fig. 1, it is shown that the ICE algorithm starts at each epoch by calculating the set of state estimation residuals

[3]The **libcluster** [31] software library was utilized to implement ICE.

[4]This whitening process is conducted because the covariance test is only valid for unit covariance matrices.

$\mathbf{R_t}$ from the current set of observations $\mathbf{Y_t}$ and the state propagated from the previous epoch $\mathbf{X_{t-1}}$. As discussed within Section III-A, this set of state estimation residuals $\mathbf{R_t}$ can be partitioned into two distinct groups (i.e., the set of state estimation residuals which correspond to erroneous observations $\mathbf{R_{O,t}}$, and the set of state estimation residuals which correspond to observations that adhere to the *a priori* model $\mathbf{R_{I,t}}$) through the utilization of the z-test.

With the set $\mathbf{R_{O,t}}$, the previous set of state estimation residuals which correspond to erroneous observations $\mathbf{R_O}$ is appended. If the length of $\mathbf{R_O}$ is greater than a user defined threshold[5] (i.e., if $|\mathbf{R_O}| > T_c$), the set is utilized to modify the measurement uncertainty model, as described in Section III-B. After the adaptation of the uncertainty model, the set $\mathbf{R_O}$ is cleared and the set of observations which adhere to the *a priori* model $\mathbf{R_{I,t}}$ are incorporated. With the incorporation of the new observations, a new state estimate is provided, following the discussion provided in Section II-B.

If the length of set of state estimation residuals, which correspond to erroneous observations, $\mathbf{R_O}$ is less than a user defined threshold, then the uncertainty model is not adapted for the current epoch. Instead, the previous measurement uncertainty model is utilized to incorporate the new set of observations which adhere to the *a priori* model. With the new observations incorporated, a new state estimated is provided, as described in Section II-B. This process is continued in an iterative fashion for as long as needed (e.g., until the data collection terminates).

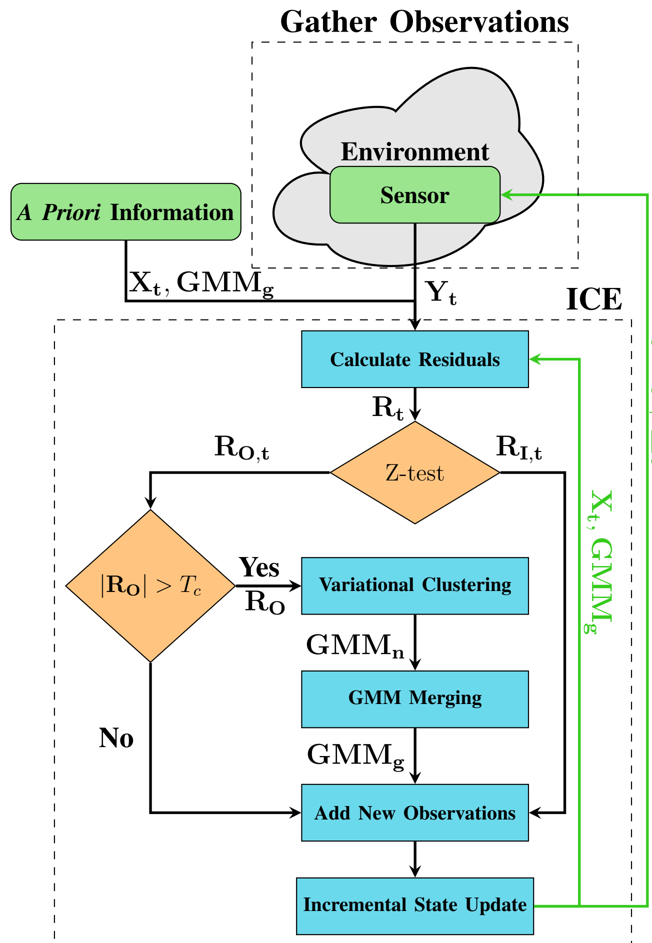

Fig. 1: Graphical depiction of the proposed robust state estimation algorithm titled incremental covariance estimation (ICE).

IV. RESULTS

A. Data Collection

To conduct an evaluation of the proposed robust estimation framework, a collection of three kinematic GNSS data sets is utilized. These GNSS data sets, as can be visualized through their ground traces, which are shown in Fig. 2, were made publicly available and are described within [19].

For these data collects, the binary in-phase and quadrature (IQ) data in the L1-band was recorded. By recording the IQ data in place of the GNSS receiver dependent observations (i.e., the pseudorange and carrier-phase observables), the same data collect can be utilized to generate several sets of observations with varying levels of degradation after playing back through a software defined GNSS receiver [35] with different sets of tracking parameters. Specifically, the receiver dependent observations can be generated off-line by playing the IQ data into a GNSS receiver, where the level of degradation is varied by changing the GNSS receiver's tracking parameters (i.e., changing the bandwidth of the phase lock loop (PLL), the delay lock loop (DLL) and the correlator spacing). For a detailed discussion on the impact that the GNSS receiver tracking parameters can have on the quality of the generated observables, the reader is referred to [36], [37], which is reviewed in [19].

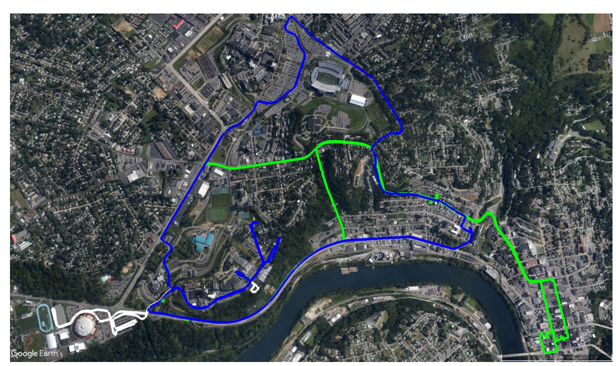

Fig. 2: Ground trace for the three utilized GNSS data sets. The white trace corresponds to data collect 1, the green trace corresponds to data collect 2, and the blue trace corresponds to data collect 3.

For this study, two sets of observations are generated (i.e., a low-quality and high-quality data set) for each of the data collects. The specific GNSS receiver tracking parameters utilized to generate the low-quality and high-quality observations are provided within Table III of [19].

[5]The specific realization of this threshold has the potential to greatly affect the estimation accuracy, and run-time performance of the ICE algorithm. Within this study, T_c was set to $1,000$ as that provided an acceptable compromise between run-time performance and the covariance estimation accuracy of the VI algorithm for a 2-dimensional covariance model. A thorough sensitivity analysis of the ICE approach will be the subject of a future study.

B. Factor Graph Construction

The specific factor graph construction, utilized to enable GNSS based inference in this evaluation, is adopted from [38]. Thus, a detailed review of the utilized construction has been omitted from this paper; however, for a succinct review of the utilized GNSS observation model, and the utilized method for incorporating GNSS observation into the factor graph, the reader is referred to Section II of [38]. Aside from the GNSS observations, the only other information incorporated in the factor graph is a process noise constraint between consecutive state estimates.

C. Evaluation

With the discussed GNSS observations and the specific factor graph construction, an evaluation of the proposed methodology can be conducted. To provided a comparison for the proposed approach, four additional estimation frameworks will be utilized. The first comparison methodology is the traditional l^2-norm based estimator. The second comparison methodology is the MM approach, which has a static measurement error covariance model (i.e., a fixed two component measurement error covariance model). The third comparison methodology is the DCS approach, where the DCS approach is utilized because it is both a closed form version of switchable constraints and a specific implementation of an m-estimator [13]. All of the above disused robust estimators are built upon the iSAM2 algorithm [21], as implemented within the Georgia Tech Smoothing and Mapping (**GTSAM**) library [39]. As a final method of comparison, the BCE [19] approach is utilized.

All of the utilized estimation frameworks are provided the same initial measurement covariance model (i.e., $\Lambda_o = \text{diag}(2.5^2, 0.25^2)$). Additionally, the estimator specific hyper-parameters utilized within this evaluation are provided in Table I.

TABLE I: Robust optimization parameter definition, where K_ρ and K_Φ are the DCS pseudorange and carrier-phase observation kernel widths, respectively.

Methodology	Parameter	Value
DCS	K_ρ	2.5
	K_Φ	0.25
MM	weighting	1
	scale factor	10
ICE	T_c	$1,000$
	T_r	3.0

1) Localization Performance: To enable the assessment of the localization performance, a reference ground-truth must be established. To generate this ground-truth, a differential GNSS solution (i.e., real time kinematic (RTK)[6]) is utilized, which is known to provide centimeter level localization accuracy [36].

With the RTK generated reference ground-truth solution, the localization performance – as quantified through the residual-sum-of-squares (RSOS) positioning error – of the five estimation frameworks, when low-quality observations are utilized, is provided in Table II. From Table II, it can be seen that all four of the robust estimation frameworks provided a significant increase is localization accuracy, with respect to the median, when compared to the traditional l^2-norm approach.

Additionally, it should be noted that the ICE approach provides the most accurate, with respect to median error, solution for all three data collects when low-quality observations are utilized. At first, it may seems counterintuitive that the ICE implementation out-performs the BCE algorithm with respect to median positioning error; however, this result is expected as the ICE algorithm is initially rejecting observations that do not adhere to the observation model (i.e., the ICE algorithm does not include erroneous observations within optimization, instead, it utilizes those observation to adapt the measurement covariance model). On the other hand, the BCE approach never rejects observations (i.e., all observations are utilized during optimization), thus creating a possibility to bias in the solution.

To continue the localization performance evaluation, we can assess the localization performance of the four estimation frameworks with the high-quality observations, as provided in Table III. From Table III, first, it should be noted that all four estimation frameworks are providing comparable localization statistics – as would be expected when the utilized observations adhere to the *a priori* measurement error covariance model. However, it can also be noted that the ICE approach is providing the most accurate localization statistics, for the incremental estimation algorithms, the majority of the time.

2) Covariance Estimation Analysis: To continue the evaluation, the estimated covariance from the ICE approach is assessed. Within this assessment, we have two primary objectives. First, we would like to show that the incrementally estimated covariance represents the measurement uncertainty model. Secondly, we would like to show that the covariance estimation process is efficiently conducted.

To enable this assessment the high-quality observations are utilized, as provided in Fig. 3. Within Fig. 3, the black points correspond to the state estimation residuals of observations which sufficiently adhere to the *a priori* measurement error uncertainty model. While, the red points correspond to the state estimation residuals of observations which were not well defined by the *a priori* measurement uncertainty model, and thus not included during optimization; however, were utilized to modify the measurement uncertainty model. Additionally, the ellipses correspond to components of the incrementally estimated measurement error uncertainty model, with 95% confidence.

From Fig. 3, it can be seen that the incrementally estimated measurement uncertainty models closely resemble the assumed model for the high quality observations (i.e., an inlier distribution which characterizes a majority of the observations, and outlier distributions which characterize a small percentage of erroneous observations). This is specifically evident for data collects 1 and 3, as depicted in Fig. 3a and Fig. 3c, respectively.

To verify the efficiency of the covariance adaptation approach, we can evaluate the number of times the measurement uncertainty model was adapted. For, data collects 1 and 3, as depicted in Fig, 3a and Fig. 3c, the covariance model

[6]This solution was realized with **RTKLIB** [40].

TABLE II: Horizontal RSOS localization error results when low fidelity receiver tracking parameters are utilized to generate the observations. The green and red cell entries correspond to the minimum and maximum statistic for the incremental estimation frameworks, respectively. As a comparison to the incremental estimators, the positioning performance provided by the previously proposed BCE approach is provided.

(a) Localization results for data collect 1.

(m.)	L_2	DCS	MM	ICE	BCE
mean	2.51	0.99	1.66	0.73	1.12
median	2.57	0.64	1.63	0.56	1.05
std. dev.	1.41	0.98	1.05	0.72	0.40
max	10.78	9.71	10.06	13.19	6.36

(b) Localization results for data collect 2.

(m.)	L_2	DCS	MM	ICE	BCE
mean	4.00	4.00	3.12	2.11	2.86
median	2.48	2.08	1.94	0.93	1.78
std. dev.	3.87	4.59	3.92	2.10	1.90
max	29.18	31.05	31.40	23.02	11.16

(c) Localization results for data collect 3.

(m.)	L_2	DCS	MM	ICE	BCE
mean	4.94	4.16	4.51	4.35	4.83
median	4.41	2.82	3.62	1.48	5.54
std. dev.	2.97	3.54	3.33	5.23	2.08
max	29.53	30.38	28.30	26.61	10.45

TABLE III: Horizontal RSOS localization error results when high fidelity receiver tracking parameters are utilized to generate the observations. The green and red cell entries correspond to the minimum and maximum statistic for the incremental estimation frameworks, respectively. As a comparison to the incremental estimators, the positioning performance provided by the previously proposed BCE approach is provided.

(a) Localization results for data collect 1.

(m.)	L_2	DCS	MM	ICE	BCE
mean	0.44	0.43	0.41	0.42	0.64
median	0.37	0.36	0.35	0.35	0.66
std. dev.	0.30	0.27	0.29	0.28	0.42
max	5.38	5.33	5.35	5.22	6.04

(b) Localization results for data collect 2.

(m.)	L_2	DCS	MM	ICE	BCE
mean	0.79	0.81	0.84	0.79	0.58
median	0.82	0.81	0.84	0.83	0.56
std. dev.	0.46	0.46	0.50	0.46	0.40
max	3.97	3.93	10.77	2.95	3.91

(c) Localization results for data collect 3

(m.)	L_2	DCS	MM	ICE	BCE
mean	1.09	1.10	1.11	1.07	0.90
median	0.96	0.95	1.00	0.89	0.82
std. dev.	0.67	0.73	0.72	0.66	0.38
max	7.83	7.83	18.08	7.82	3.67

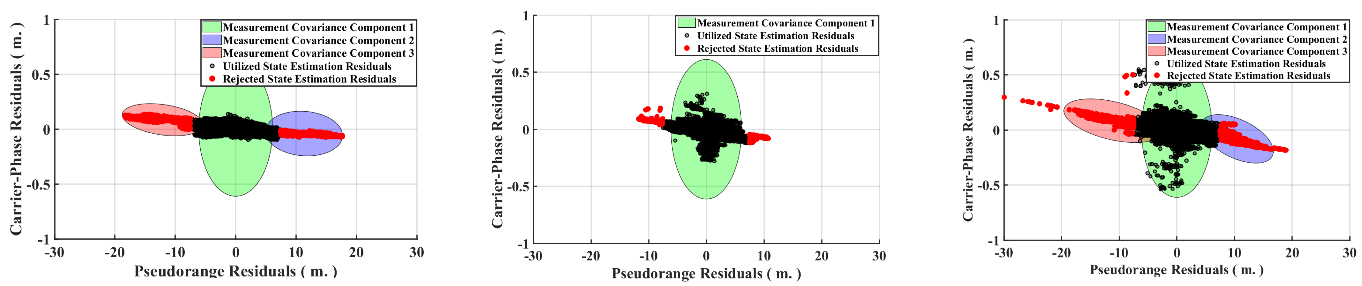

(a) Incrementally estimated measurement error covariance model for data collect 1. For this measurement uncertainty model, approximately 91% of the observations are characterized by component 1.

(b) Incrementally estimated measurement error covariance model for data collect 2. For this data collect, only 249 observations did not adhere to the *a priori* measurement uncertainty model.

(c) Incrementally estimated measurement error covariance model for data collect 3. For this measurement uncertainty model, approximately 98% of the observations are characterized by component 1.

Fig. 3: Incrementally estimated measurement error covariance model when the observations are generated with high fidelity receiver tracking parameters.

was only adapted once to enable the incorporation of two outlier distributions. For data collect 2, as depicted in Fig. 3b, no covariance adaptation step was conducted – instead, only 249 observations were rejected. In contrast, if the covariance model was naively adapted every time the number of residuals were greater than the residual cardinality threshold, then data collect 1 would have required 75 adaptations, data collect 2 would have required 57 adaptations, and data collect 3 would have required 91 adaptations. Thus, the incorporation of the z-test to partition the set of residuals dramatically increased the efficiency of the proposed approach.

3) Run-time Analysis: To conclude the evaluation of the proposed methodology, a run-time comparison[7] for all of the incremental estimators is provided in Fig 4. From Fig. 4, it is shown that l^2-norm, DCS, and the MM approaches all provide comparable run-time performance.

In Fig. 4 it is clearly shown that the ICE methodology provides the slowest average run-time; however, this slower run-time – which is still on average approximately 25 Hz – could prove to be a valid comprise when considering the significantly increase in localization accuracy granted by the approach. Additionally, although ICE approach is the slowest, while not exploited in this current implementation, it is possible to implement the algorithm such that covariance adaption and state estimation are running in parallel.

V. Conclusion

Within this paper, we propose a novel extension to the measurement uncertainty model estimation paradigm for enabling robust state estimation. Specifically, we propose an efficient, incremental extension of the methodology. The efficiency of the approach is granted by adapting the uncertainty model with only a small subset of informative state estimation residuals (i.e., the state estimation residuals which do not adhere to the *a priori* model). The incremental nature of the approach is granted through recent advances within the probabilistics graphical model community, and the ability to merge GMM's.

[7]This run-time comparison was conducted on a 2.8GHz Intel Core i7-7700HQ processor.

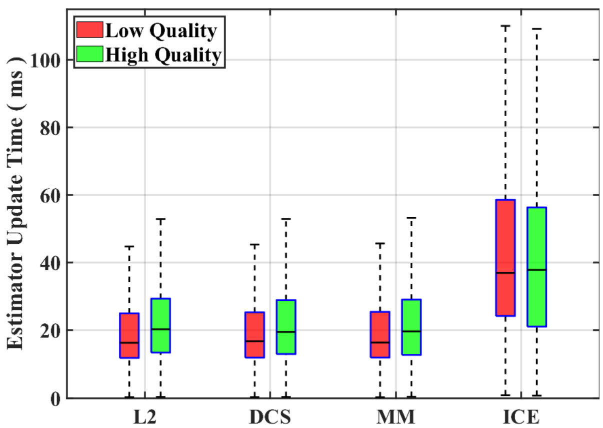

Fig. 4: Estimator update time in milliseconds for each of the incremental estimation frameworks over all data collects.

To evaluate the proposed ICE approach, three degraded GNSS data sets are utilized. Based upon the results obtained on these data sets, the proposed approach provides promising results. Specifically, the proposed ICE approach provides significantly increased localization performance when utilizing degraded data, when compared to other state-of-the-art robust, incremental estimation algorithms.

REFERENCES

[1] D. Simon, *Optimal state estimation: Kalman, H infinity, and nonlinear approaches*. John Wiley & Sons, 2006.

[2] R. E. Kalman, "A new approach to linear filtering and prediction problems," *Journal of basic Engineering*, vol. 82, no. 1, pp. 35–45, 1960.

[3] S. Thrun, W. Burgard, and D. Fox, *Probabilistic robotics*. MIT press, 2005.

[4] F. R. Hampel, "Contribution to the theory of robust estimation," *Ph. D. Thesis, University of California, Berkeley*, 1968.

[5] J. Hidalgo-Carrió, D. Hennes, J. Schwendner, and F. Kirchner, "Gaussian process estimation of odometry errors for localization and mapping," in *2017 IEEE International Conference on Robotics and Automation (ICRA)*, pp. 5696–5701, IEEE, 2017.

[6] T. Tang, D. Yoon, F. Pomerleau, and T. D. Barfoot, "Learning a bias correction for lidar-only motion estimation," in *2018 15th Conference on Computer and Robot Vision (CRV)*, pp. 166–173, IEEE, 2018.

[7] P. J. Huber, *Robust Statistics*. Wiley New York, 1981.

[8] A. Kvas and T. Mayer-Gürr, "Grace gravity field recovery with background model uncertainties," *Journal of geodesy*, vol. 93, no. 12, pp. 2543–2552, 2019.

[9] Y. Latif, C. Cadena, and J. Neira, "Realizing, reversing, recovering: Incremental robust loop closing over time using the irrr algorithm," in *2012 IEEE/RSJ International Conference on Intelligent Robots and Systems*, pp. 4211–4217, IEEE, 2012.

[10] E. Olson, M. R. Walter, S. J. Teller, and J. J. Leonard, "Single-cluster spectral graph partitioning for robotics applications.," in *Robotics: Science and Systems*, pp. 265–272, 2005.

[11] L. Carlone, A. Censi, and F. Dellaert, "Selecting good measurements via âĎŞ 1 relaxation: A convex approach for robust estimation over graphs," in *2014 IEEE/RSJ International Conference on Intelligent Robots and Systems*, pp. 2667–2674, IEEE, 2014.

[12] N. Sünderhauf and P. Protzel, "Switchable constraints for robust pose graph SLAM," in *2012 IEEE/RSJ International Conference on Intelligent Robots and Systems*, pp. 1879–1884, IEEE, 2012.

[13] P. Agarwal, G. D. Tipaldi, L. Spinello, C. Stachniss, and W. Burgard, "Robust map optimization using dynamic covariance scaling," in *2013 IEEE International Conference on Robotics and Automation*, pp. 62–69, Citeseer, 2013.

[14] E. Olson and P. Agarwal, "Inference on networks of mixtures for robust robot mapping," *The International Journal of Robotics Research*, vol. 32, no. 7, pp. 826–840, 2013.

[15] R. M. Watson, C. N. Taylor, R. C. Leishman, and J. N. Gross, "Batch Measurement Error Covariance Estimation for Robust Localization," in *Proceedings of the 31st International Technical Meeting of The Satellite Division of the Institute of Navigation (ION GNSS+2018)*, pp. 2429–2439, 2018.

[16] T. Pfeifer and P. Protzel, "Robust sensor fusion with self-tuning mixture models," in *2018 IEEE/RSJ International Conference on Intelligent Robots and Systems (IROS)*, pp. 3678–3685, IEEE, 2018.

[17] D. Wang, J. Xue, Z. Tao, Y. Zhong, D. Cui, S. Du, and N. Zheng, "Accurate mix-norm-based scan matching," in *2018 IEEE/RSJ International Conference on Intelligent Robots and Systems (IROS)*, pp. 1665–1671, IEEE, 2018.

[18] G. Agamennoni, P. Furgale, and R. Siegwart, "Self-tuning m-estimators," in *2015 IEEE International Conference on Robotics and Automation (ICRA)*, pp. 4628–4635, IEEE, 2015.

[19] R. M. Watson, J. N. Gross, C. N. Taylor, and R. C. Leishman, "Enabling Robust State Estimation through Measurement Error Covariance Adaptation," *IEEE Transactions on Aerospace and Electronic Systems*, pp. 1–1, 2019.

[20] T. Pfeifer and P. Protzel, "Incrementally learned mixture models for gnss localization," *arXiv preprint arXiv:1904.13279*, 2019.

[21] M. Kaess, H. Johannsson, R. Roberts, V. Ila, J. J. Leonard, and F. Dellaert, "iSAM2: Incremental smoothing and mapping using the Bayes tree," *The International Journal of Robotics Research*, vol. 31, no. 2, pp. 216–235, 2012.

[22] M. Song and H. Wang, "Highly efficient incremental estimation of Gaussian mixture models for online data stream clustering," in *Intelligent Computing: Theory and Applications III*, vol. 5803, pp. 174–184, International Society for Optics and Photonics, 2005.

[23] F. Dellaert, M. Kaess, *et al.*, "Factor graphs for robot perception," *Foundations and Trends® in Robotics*, vol. 6, no. 1-2, pp. 1–139, 2017.

[24] F. Dellaert and M. Kaess, "Square Root SAM: Simultaneous localization and mapping via square root information smoothing," *The International Journal of Robotics Research*, vol. 25, no. 12, pp. 1181–1203, 2006.

[25] M. Kaess, A. Ranganathan, and F. Dellaert, "Fast Incremental Square Root Information Smoothing.," in *IJCAI*, pp. 2129–2134, 2007.

[26] G. H. Golub and C. F. van Loan, *Matrix Computations*. JHU Press, fourth ed., 2013.

[27] M. Kaess, V. Ila, R. Roberts, and F. Dellaert, "The Bayes tree: An algorithmic foundation for probabilistic robot mapping," in *Algorithmic Foundations of Robotics IX*, pp. 157–173, Springer, 2010.

[28] Z. Zhang, "Parameter estimation techniques: A tutorial with application to conic fitting," *Image and vision Computing*, vol. 15, no. 1, pp. 59–76, 1997.

[29] D. M. Blei, M. I. Jordan, *et al.*, "Variational inference for Dirichlet process mixtures," *Bayesian analysis*, vol. 1, no. 1, pp. 121–143, 2006.

[30] M. Beal, *Variational algorithms for approximate Bayesian inference*. PhD thesis, University of London, 2003.

[31] D. Steinberg, *An unsupervised approach to modelling visual data*. PhD thesis, University of Sydney., 2013.

[32] A. Doucet and X. Wang, "Monte Carlo methods for signal processing: a review in the statistical signal processing context," *IEEE Signal Processing Magazine*, vol. 22, no. 6, pp. 152–170, 2005.

[33] O. Ledoit, M. Wolf, *et al.*, "Some hypothesis tests for the covariance matrix when the dimension is large compared to the sample size," *The Annals of Statistics*, vol. 30, no. 4, pp. 1081–1102, 2002.

[34] H. Hotelling, "The generalization of StudentâĂŹs ratio," in *Breakthroughs in statistics*, pp. 54–65, Springer, 1992.

[35] C. Fernandez-Prades, J. Arribas, P. Closas, C. Aviles, and L. Esteve, "GNSS-SDR: an open source tool for researchers and developers," in *Proceedings of the 24th International Technical Meeting of The Satellite Division of the Institute of Navigation (ION GNSS 2011)*, pp. 780–0, 2001.

[36] E. Kaplan and C. Hegarty, *Understanding GPS: principles and applications*. Artech house, 2005.

[37] A. Van Dierendonck, P. Fenton, and T. Ford, "Theory and performance of narrow correlator spacing in a gps receiver," *Navigation*, vol. 39, no. 3, pp. 265–283, 1992.

[38] R. M. Watson and J. N. Gross, "Evaluation of kinematic precise point positioning convergence with an incremental graph optimizer," in *Position, Location and Navigation Symposium (PLANS), 2018 IEEE/ION*, pp. 589–596, IEEE, 2018.

[39] F. Dellaert, "Factor graphs and gtsam: A hands-on introduction," tech. rep., Georgia Institute of Technology, 2012.

[40] T. Takasu, "RTKLIB: An open source program package for GNSS positioning," 2011.